

Simulation of the temperature-dependent resistivity of $\text{La}_{1-x}\text{Te}_x\text{MnO}_3$

Dong-yi Guan, Qing-li Zhou, Kui-juan Jin*, Guo-tai Tan, Zheng-hao Chen, Hui-bin Lu, Bo-lin Cheng, Yue-liang Zhou, Meng He, Peng Han, and Guo-zhen Yang

Beijing National Laboratory for Condensed Matter Physics, Institute of Physics, Chinese Academy of Science, P.O. Box 603, Beijing 100080, P.R. China

Received 22 March 2005, revised 29 July 2005, accepted 22 August 2005
Published online 20 October 2005

PACS 72.10.Bg, 72.80.Ga, 75.47.Lx

The resistivity ρ of $\text{La}_{1-x}\text{Te}_x\text{MnO}_3$ ($x = 0.1, 0.14$) is studied using a random resistor network, based on phase separation between ferromagnetic (FM) and paramagnetic (PM) domains. By considering the irregular shape of the domains, a revised method, which is used to find the shortest paths across the sample, leads to a good agreement between the simulated results and experiment data. Moreover, it is found that FM components increase with Te doping, leading to a reduction of the resistivity and a shift of the transition temperature. This method is proved to be valid and the phase separation scenario is shown theoretically to be good enough in describing the electrical conductivity of the doped manganese perovskites.

© 2005 WILEY-VCH Verlag GmbH & Co. KGaA, Weinheim

1 Introduction

Considerable work is currently being focused on the study of doped manganese perovskites [1, 2]. These materials have unexplained transport properties. They are insulators at room temperature, changing into conductors at low temperature. A sharp peak in the resistivity ρ appears at the ferromagnetic (FM)-paramagnetic (PM) transition. The transition temperature is denoted T_{MI} . The phase separation phenomenon has been observed in many doped manganese perovskites, such as $\text{La}_{1-x}\text{Ca}_x\text{MnO}_3$ [3], $(\text{La},\text{Pr},\text{Ca})\text{MnO}_3$ [4], and $\text{La}_{1-x}\text{Te}_x\text{MnO}_3$ [5].

In the present paper, we present a new calculation method to simulate the relation between ρ and temperature T of $\text{La}_{1-x}\text{Te}_x\text{MnO}_3$ by introducing the breadth-first traversal (BFT) algorithm based on the phase-separated framework and the random resistor network model. This method can give good results with much less calculation effort so that it is much more convenient than the traditional method of solving the Kirchhoff equations for the resistor network, as reported in the early literature [6–8].

2 Model and method

The main concept in the random resistor network model is summarized in Fig. 1. We assume the sample to be mixed by FM and PM domains, which are regarded as squares. The FM and PM squares have metallic and insulating properties, respectively (Fig. 1a). Each FM or PM square is assumed to have a resistance of r_m or r_i and then the sample can be considered as a network of resistors. In our network, there are connected insulating or metallic paths across the sample. The resistance of the whole insulating (R_i) or

* Corresponding author: e-mail: kjjin@aphy.iphy.ac.cn

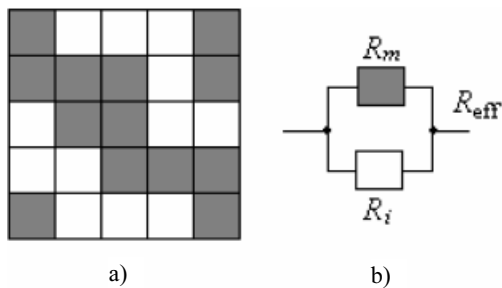


Fig. 1 a) Schematic of random resistor network model. Gray squares represent metallic domains and white ones represent insulating domains. b) Two-resistance model for doped manganese perovskites. Effective resistance R_{eff} arises from the parallel connection of metallic R_m and insulating R_i resistances.

metallic (R_m) regions is assumed to be proportional to the length of the shortest insulating or metallic path. The total resistance of the sample R_{eff} can be characterized by a simple two parallel resistances description (Fig. 1b). As the temperature varies, the fraction of the insulating or metallic regions changes, and then the relation between R_{eff} and T is obtained.

Breadth-first search [9] is a traversal through a graph that touches all of the nodes reachable from a particular source node. A BFT visits nodes that are closer to the source before visiting nodes that are further away. The distance is defined as the number of edges in the shortest path from the source node. This algorithm, which explores all nodes adjacent to the current node before moving on, can be used to compute the shortest path from the source to all reachable nodes and the shortest-path distances. When properly implemented, all nodes in a given connected component are explored. Using the BFT algorithm, the path lengths of the metallic and insulating domains are found. The resistances R_m and R_i are then calculated. Finally, according to the size of the sample and the effective resistance R_{eff} , the effective resistivity ρ can be obtained. It is noticeable that this method is much more convenient than the traditional method of solving the Kirchhoff equations for the resistor network.

The resistivities of the metallic (ρ_m) and insulating (ρ_i) domains are dependent on temperature. It is reasonable to assume that they have the forms $\rho_m = \rho_{m0} + \rho_{m1}T^2 + \rho_{m2}T^{4.5}$ and $\rho_i = \rho_{i0} \exp(E_0/k_B T)$ [10], where ρ_{m0} , ρ_{m1} , ρ_{m2} , and ρ_{i0} are parameters fitted from the experimental data, and E_0 denotes the activation energy. In order to represent the indications of temperature-induced percolation, a temperature-dependent metallic fraction $p(T)$ is needed. The parameter p must decrease as T increases, and should vary rapidly near the Curie temperature T_C as does the magnetization [8].

3 Experiments and simulation

We fabricated $\text{La}_{1-x}\text{Te}_x\text{MnO}_3$ ($x = 0.1, 0.14$) using pulsed laser deposition (PLD) on (100) SrTiO_3 (STO) substrates. After deposition, the films were held at 780 °C for 30 min in high-purity oxygen at a pressure of 50 Pa, and were then postannealed at 760 °C for 8 h in flowing oxygen in order to improve the oxygen content of the thin films. The magnetic measurement was carried out using a superconducting quantum interference device magnetometer (MPMS-7) in the temperature range 5–300 K. We then measured the resistivities of $\text{La}_{0.9}\text{Te}_{0.1}\text{MnO}_3$ films in zero magnetic fields from 5 to 325 K.

In our simulation, the metallic and insulating domains are all assumed to be squares, and a 100×100 matrix is used. To simplify the problem, we first assume that two squares are connected only when they have a common edge, that is, we search a path in four directions for each square. Figure 2 shows the result of the simulation for $\text{La}_{0.9}\text{Te}_{0.1}\text{MnO}_3$ with T_C at 261 K. At low temperature the resistivity of the sample is small, as it is at room temperature. A large peak tending toward infinity appears in the intermediate temperature range from 220 to 275 K. We assume that the relation between the fraction of metallic regions and T can be described by a Fermi distribution function, which has a form similar to the magnetization–temperature relation. The relation of p – T is also shown by curve a in Fig. 3. At low temperature, there are many metallic paths across the sample for the high fraction of metallic domains, so R_m is very small. R_{eff} is mainly determined by R_m because R_m and R_i are parallel connected so that R_{eff} is also very small. It is obvious as shown by curve a in Fig. 3 that the fraction of metallic domains decreases

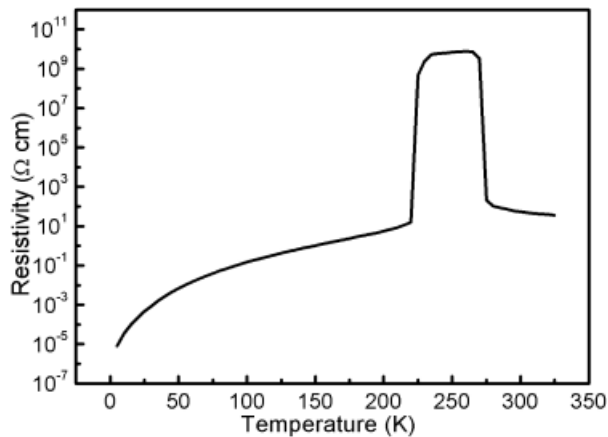


Fig. 2 Resistivity ρ vs. T , assuming that two domains are connected only when they have a common edge. A peak tending to infinity appears near T_C .

rapidly from 150 K and is less than 0.6 at 220 K. Thus there are so few metallic paths across the sample that R_m increases rapidly and R_{eff} also increases rapidly. So a peak of ρ appears near T_C . However, when the temperature increases continuously, ρ_i is smaller than ρ_m due to the exponential decay of ρ_i with increasing temperature. Therefore R_{eff} is mainly determined by R_i , and R_{eff} decreases again.

It is noted that the peak value of the resistivity tends to infinity and does not fit the experimental data. In the method to obtain Fig. 2, we only search paths in four adjacent directions for each square in the above simulation, that is, we assume that the current cannot flow through two diagonal adjacent squares. When the temperature is near T_C , the fractions of the insulating and metallic regions are almost same, and there is no path of either metallic or insulating regions across the sample, so both R_m and R_i tend to infinity. This is not realistic. In fact, the current can pass when two squares are diagonally adjacent due to percolation. It is reasonable to assume that two diagonal adjacent squares are connected as well as two exactly adjacent squares, that is, to search paths in eight directions for each square. This improvement makes the simulated results fit the experimental data better, as shown in Fig. 4. In our calculation, the activation energy E_0 is 43 meV, and the simulated ρ - T curve is plotted together with the corresponding experimental data (Fig. 4a). It can be seen that the result not only yields the M-I transition at T_C , but also fits the experimental data well over the whole temperature range studied.

The simulated results and experimental data for $\text{La}_{0.86}\text{Te}_{0.14}\text{MnO}_3$ films are shown in Fig. 4b. We find that the activation energy E_0 is 8.6 meV. It is worth noting that Te doping decreases the activation energy. The relevant p - T relation is shown as curve b in Fig. 3. By comparing curves a and b in Fig. 3, we find that the metallic fraction in $\text{La}_{0.86}\text{Te}_{0.14}\text{MnO}_3$ is larger than that in $\text{La}_{0.9}\text{Te}_{0.1}\text{MnO}_3$. The difference of

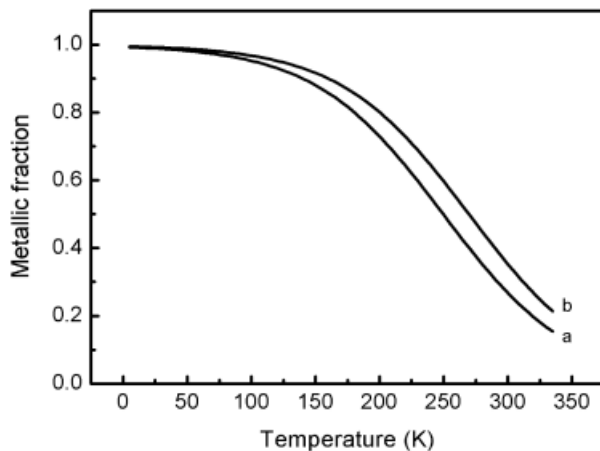


Fig. 3 Metallic fraction p vs. T : a) $\text{La}_{0.9}\text{Te}_{0.1}\text{MnO}_3$; b) $\text{La}_{0.86}\text{Te}_{0.14}\text{MnO}_3$.

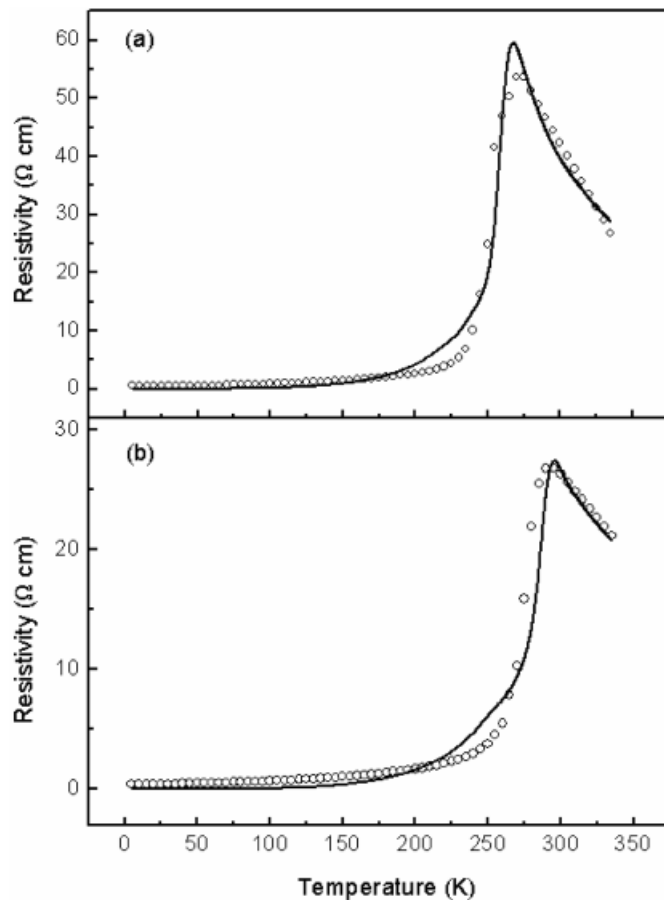


Fig. 4 Resistivity ρ vs. T , assuming that two domains are connected when they have either a common edge or a point. The open circles are experimental data and the solid curves are the simulated results: a) $\text{La}_{0.9}\text{Te}_{0.1}\text{MnO}_3$; b) $\text{La}_{0.86}\text{Te}_{0.14}\text{MnO}_3$.

$\rho(T)$ between the two curves increases with temperature, and almost reaches a constant value when the temperature is larger than T_C . The possible reason is that the amount of free electrons in the sample increases with an increase of Te doping. At low temperature, the majority of electrons are difficult to move, so the metallic fraction increases very little. As the temperature increases, more and more electrons can move easily, so the metallic fraction increases obviously. The increase of the metallic fraction shifts T_{MI} to a higher temperature and decreases the peak value of the resistivity.

4 Conclusion

The BFT algorithm is introduced to describe the transport problem and is found to be a valid algorithm from the work presented. We have simulated the temperature dependence of the resistivity in $\text{La}_{1-x}\text{Te}_x\text{MnO}_3$ ($x = 0.1, 0.14$) based on the random resistor network model. The simulated results give quantitative fits to the experimental data over the whole temperature range. The results also indicate that the activation energy in $\text{La}_{0.86}\text{Te}_{0.14}\text{MnO}_3$ is lower than that in $\text{La}_{0.9}\text{Te}_{0.1}\text{MnO}_3$ and the metallic fraction in $\text{La}_{0.86}\text{Te}_{0.14}\text{MnO}_3$ is larger than that in $\text{La}_{0.9}\text{Te}_{0.1}\text{MnO}_3$. Therefore, the resistivity of the sample is reduced and the transition temperature increases as the amount of Te increases. Furthermore, we believe that this model is also useful for further simulation work on other perovskite materials. Work to simulate the conductivity of doped manganese perovskites in applied magnetic fields is ongoing.

Acknowledgement The authors gratefully acknowledge the financial support from the National Natural Science Foundation of China.

References

- [1] Y. Tokura, Y. Tomioka, H. Kuwahara, A. Asamitsu, Y. Moritomo, and M. Kasai, *J. Appl. Phys.* **79**, 5288 (1996).
- [2] Y. Tomioka, A. Asamitsu, H. Kuwahara, Y. Moritomo, and Y. Tokura, *Phys. Rev. B* **53**, 1689 (1996).
- [3] M. Fäth, S. Freisem, A. A. Menovsky, Y. Tomioka, J. Aarts, and J. A. Mydosh, *Science* **285**, 1540 (1999).
- [4] M. Uehara, S. Nori, C. H. Chen, and S. W. Cheong, *Nature (London)* **399**, 560 (1999).
- [5] G. T. Tan, S. Dai, P. Duan, Y. L. Zhou, H. B. Lu, and Z. H. Chen, *Phys. Rev. B* **68**, 014426 (2003).
- [6] S. Kirkpatrick, *Rev. Mod. Phys.* **45**, 574 (1973).
- [7] Z. Y. Li, S. L. Yuan, G. Peng, and C. Q. Tang, *Chin. Phys. Lett.* **18**, 1392 (2001).
- [8] M. Mayr, A. Moreo, J. A. Vergés, J. Arispe, A. Feiguin, and E. Dagotto, *Phys. Rev. Lett.* **86**, 135 (2001).
- [9] S. Skiena, *Implementing Discrete Mathematics: Combinatorics and Graph Theory with Mathematica* (Addison-Wesley, CA, 1990).
- [10] A. K. Pradhan, Y. Feng, B. K. Roul, and D. R. Sahu, *Appl. Phys. Lett.* **79**, 506 (2001).